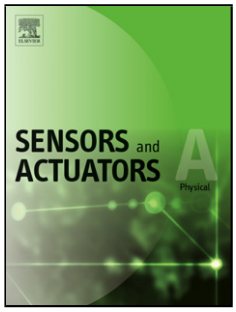

Title: Radioluminescence results from an Al_2O_3: C+fiber prototype: 6 MV medical beam

Authors: L.F. Nascimento, I. Veronese, G. Loi, E. Mones, F. Vanhavere, D. Verellen

PII: S0924-4247(17)32230-6
DOI: https://doi.org/10.1016/j.sna.2018.03.007
Reference: SNA 10673

To appear in: *Sensors and Actuators A*

Received date: 14-12-2017
Revised date: 5-3-2018
Accepted date: 7-3-2018

Please cite this article as: Nascimento LF, Veronese I, Loi G, Mones E, Vanhavere F, Verellen D, Radioluminescence results from an Al_2O_3: C+fiber prototype: 6 MV medical beam, *Sensors and Actuators: A Physical* (2010), https://doi.org/10.1016/j.sna.2018.03.007

Radioluminescence results from an Al_2O_3:C+fiber prototype: 6 MV medical beam

Nascimento, L. F.[a,b,c*]; Veronese, I[d]; Loi, G.[e]; Mones, E.[e]; Vanhavere, F.[b]; Verellen, D.[c]

[a] Gent University, Department Radiotherapy and Experimental Cancer Research, De Pintelaan, 185. 9000 Gent, Belgium
[b] SCK•CEN Belgian Nuclear Research Centre, Boeretang 200, Mol, Belgium
[c] University of VUB, UZ Brussel, Radiotherapie, Groep Medische Fysica, Brussels, Belgium
[d] Dipartimento di Fisica, Università degli Studi di Milano and INFN, Via Celoria 16, 20133 Milano, Italy
[e] Medical Physics Department, Azienda Ospedaliero Universitaria Maggiore della Carità, Novara, Italy
**ldfnasci@sckcen.be*

Highlights

- Droplets composed of thin powder of Al_2O_3:C were prepared using a photo-curable polymer and present high spatial resolution.
- Droplets coupled to optical fibres are suitable for 1D real time dosimetry in radiotherapy beams
- The small size of droplets makes it suitable for small field size measurements and FFF modes.

The Investigations of this article focus on the response of an Al_2O_3:C radioluminescence (RL) prototype for medical dosimetry in a 6 MV photon beam. The prototype can be configured using two types of detectors coupled to fiber-optic cables - single crystal (1x1x2 mm^3) and droplets (in two grain sizes, 38 and 4μm, molded in r = 0.5 mm, l = 200 μm). By using the appropriate filters in addition to time gating it is possible to remove disturbance present during irradiation: the stem effect. Pre-irradiation of the dosimeters to a dose of 300 Gy made the memory effects in Al_2O_3:C negligible, so as to not impair the dosimetric properties of the system. The key findings are that the system is suitable for small field beam dosimetry, while giving overall good dose response in other features (i.e., beam profile, dose rate - FF and FFF modes). The results show that our prototype can be used for real time dose rate assessment in medical photon dosimetry without many correction factors. The 4μm RL measurement results are in excellent agreement (i.e. below 1%) with the dose delivered according to standard beam data.

1. Introduction:

Evolution in technology has changed radiation therapy to a highest degree of sophistication and complexity that needs to be accordingly translated to radiation protection and dosimetry. Among the innovations on treatments, flattening filter free (FFF) beams are now commonly available with new standard linear accelerators. These beams give recognized clinical advantages such as the reduced beam-on times for high dose per fraction treatments [1]. Additionally, the new systems are also capable of delivering high focalized dose distributions using small field sizes to the tumor, decreasing lateral doses to health tissues. A small field is generally defined as having dimensions smaller than the lateral range of the charged particles that contribute to the dose deposited at a point along the central axis, i.e. < 3cm^2 [2, 3].

Flattening filter free (FFF) beams and dynamic multi-leaf collimation bring new challenges on dosimetric aspects linked to field size, penumbra and quality assurance (QA) [1]. Dosimetry in small fields, for instance, is complicated [4], because most of the reference conditions parameters such as

stopping power ratio, perturbation correction, fluence and gradient corrections are not applicable [5].

A lot of effort has been dedicated on finding suitable dosimetric solutions for new and sophisticated radiotherapy treatments. Among the attempts, real-time detectors are strong candidates for the job. Real-time detectors are capable of measuring the total dose during a treatment session, but are in principle also capable to measure the time-resolved intra-fraction dose delivery (dose rate), which provides additional useful information in some situations [6].

Real-time dosimeters include ionization chambers, diodes [7], metal-oxide semiconductor field effect transistors (MOSFETs) [8], scintillation detectors [9, 10], and electronic portal imaging devices (EPIDs) [11]. Current real time techniques have inherent limitations, such as narrow dynamic range, energy dependence, processor dependence, variation in optical density or limited resolution and very high cost for hardware and labor related [12, 13]. Improvement of existing systems, as well as new solutions, is the subject of several on-going studies.

In the last two decade, optical fiber systems based on organic and inorganic materials appeared as a solution for *in vivo* radiotherapy dosimetry, with many advantages over currently employed clinical dosimetry systems. There are a number of different materials evaluated for punctual real time dose rate measurements. Among them is worth citing plastic scintillators [14-19], Ce, Cu, Ge, Eu and Yb-doped optical fibers [10, 20-24], organic scintillators [25, 26] and solid state dosimeters, such as BeO [27], LiF [16] and Al_2O_3:C [28, 29].

Al_2O_3:C optically stimulated dosimeters have been introduced in medical dosimetry of low and high LET beams [30, 31] in the past 15 years. In addition, Al_2O_3:C detectors can also be used as real time dosimeters, because the material emits radioluminescence (RL) during irradiation of which the intensity is proportional to the beam's dose rate [6]. Radioluminescence is light generated by free charge (electrons and holes induced by ionizing radiation) recombining at luminescence centers. In the case of Al_2O_3:C two RL components are present: 28 μs ('fast' component, with main emission at 520 nm) and 35 ms ('slow' component, with main emission at 420 nm) [32, 33]. Dosimetric characteristics of Al_2O_3:C radioluminescence were already demonstrated in some previous works [28, 34-39].

The protocol used in this article proposes to perform dosimetry using solely the RL from saturated (i.e. pre-irradiated) Al_2O_3:C droplets and crystals attached to optical fibers, avoiding optical stimulation, which disturbs the equilibrium of trapped charges in the crystal [35]. In this approach, Al_2O_3:C is used as a scintillator exploiting the slow component of the RL signal.

The present work investigates the performance of Al_2O_3:C RL + fiber detectors [40] using 6 MV photon beams. Results about stem effect removal, dose rate dependence in FF and FFF modalities, linearity with dose, output factors (from 1x1 cm^2 up to 30x30 cm^2), and dose profiles are presented and compared with those of standard dosimetry systems (ionization chambers and a commercial optical-fiber scintillator [31]). In addition, we discuss accuracy and precision of the RL measurements when using two different droplets (crystal sizes) vs. single crystal.

2. Materials and methods

2.1. Dosimeters and readout system

The three active dosimeters used in this work are based on 1) a 1x1x2 mm^3 single crystal ('CG'), 2) a droplet (*r*= 0.5 mm and *l*=200μm) with average crystal size of 38 μm ('38μm'), [41] and 3) a droplet (*r*= 0.5 mm and *l*=200μm) with average crystal size of 4 μm ('4μm'). In all cases we used a 15m long PMMA (GH4001) optical fiber 'glued' to the dosimeters using a photocuring polymer [41]. The bare end of each fiber was polished and glued to a SMA connector. The detectors and optical fibre were covered with a water-equivalent material to prevent light exposure.

Radioluminescence of Al_2O_3:C is known to be affected by memory effects and after-glow phenomena, as observed previously by various authors [42, 43]. These effects, if not properly taken into account,

may represent potential source of systematic errors in dose assessments by RL measurements. As observed by Andersen and colleagues [35], a proper pre-irradiation of the material enables to achieve a constancy of the RL sensitivity, provided that the Al_2O_3:C crystal is not perturbed by optical stimulation (i.e. by OSL measurements).
On the basis of these evidences, all our dosimeters were pre-saturated once with a dose of 300 Gy using a $^{90}Sr/^{90}Y$ source to fill deep traps that compete with recombination centers and the readout system was solely used in RL mode.
To assess the calibration curves of each dosimeter+fiber we previously measured the radioluminescence signal (RL_{ref}) versus reference absorbed dose (D_{ref}) with various doses of a 6 MV photon beam, 10 cm x 10 cm field size, Source Surface Distance (SSD) of 100 cm, at 10 cm depth in a PMMA slab phantom.
The readout system prototype [37] consists of an optical apparatus with focusing lenses, dichroic mirror to guide the luminescence from the optical fiber; two sets of filters, used separately, where the first (F1) rest in two 7.5 mm Hoya U-340 (Edmund Optics) for OSL measurements [29], and the second, (F2) rest in two 425 nm Hard Coated Broadband Bandpass Interference Filter (Full Width-Half Max FWHM of 25 nm, Edmund Optics) used in RL measurements. Luminescence was measured using a bialkali photomultiplier tube (PMT) (P30USB, Sens-TechTM). Data acquisition and control were performed using a NI USB 6341 card (National Instruments, USA) and a Labview program. The system is sketched in Figure 1.
In the following graphs, some results are compared with their “residuals”, defined as the difference between the observed/measured value and the predicted/reference value.

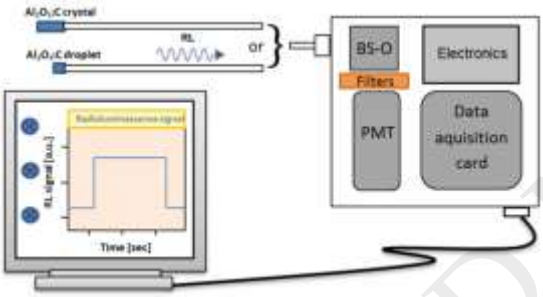

Figure 1. Sketch of the RL dosimetry system as described in the text. Two choices of RL detectors (crystal or droplet) can be coupled to the system via an optical fiber, that guides the signal thought an optical arrangement (beam splitter and focusing lenses, called BS-O), reaching the PMT tube after passing a set of filters. The signal is then processed by the DAQ and is acquired by a computer, with Labview software.

2.2. Irradiations

The external beam irradiations were performed at two different hospitals: (1) Algemeen Stedelijk Hospital (UZBrussel, Aalst/Belgium), using a 6MV beam Elekta Compact system (Elekta AB, Sweden) and; (2) University Hospital "Maggiore della Carità" (Novara, Italy) using a 6 MV x-rays beam generated by a Varian Trilogy TX accelerator (Varian Medical Systems Inc., CA, USA). Both the LINACs were calibrated following the IAEA TRS-398 code of practice (IAEA 2000) to obtain an equivalence of 1 cGy/1 monitor unit (MU) in the reference conditions, for a 10 cm × 10 cm field size, and a 100 cm source-to-surface phantom distance (10 cm depth in water). The various measurements were carried out in a water phantom (Blue Phantom, IBA Dosimetry GmbH, Germany), in a solid-water phantom (type CTG-457, Gammex, USA) and in a PMMA slab phantom. The standard beam data used as reference in this study were obtained in a water phantom with different ionization chambers and an Exradin W1 Scintillator. In particular, output factors for field sizes ranging from 1x1 to 7x7 cm^2 were obtained with a micro-ionization chamber (PTW PinPoint, TW31016, 0.016 cm^3) [44] together with an Exradin W1 Scintillator, while a Farmer IC (PTW Farmer, while a TW 30013, 0.6 cm^3) [45] was used for larger fields (7x7 – 30x30 cm^2). The beam profiles were measured with the PTW semiflex ionization chamber (TW 31010, 0.125 cm^3).

2.3. Stem effect

The stem effect, i.e. the signal generated by ionizing radiation in the optical fiber during irradiation, is an additional signal component in all real-time dosimetric measurements that involves a detector (e.g. Al_2O_3:C) connected to a light guide (optical fiber). The two main contributions to the stem effect observed in Al_2O_3:C+fibers come from Cerenkov radiation [46] and from fluorescence of water; a deduction consistent with the known high H_2O and OH content of the PMMA fibers.
To account for the stem effect we rely on both filter package (F2), centered on the main peak of the Al_2O_3:C RL 'slow' component, and on optimizing the sampling procedure. In particular, the RL signals were acquired within temporal windows of 10 ns with a frequency of 200 Hz. Since in Linacs, the maximum number of pulse/sec is set to 360 (pulse duration of few μs), sampling occurred in the time interval between Linac pulses (i.e. in the time regions where the stem effect is no more present due to the short lifetime, but where the tail of the RL signal is still measurable). This method for avoiding the stem effect was validated by using the phantom plate required for the initial calibration of the Exradin W1 Scintillator, shown in figure 2. The dosimeters were placed in the center of a radiation field with size 30x30 cm^2. Initially the fiber was stretched out of the field, thus exposing to the beam a portion of approximately 15 cm (short configuration). Afterwards, a length of fiber of 90 cm was irradiated by bending it into the track of the calibration plate (long configuration). The measurements were performed in these two different set up using the various dose rates available with the Varian accelerator in the FFF modality.
Furthermore, in order to check the Al_2O_3:C RL emission and compare it with the spectrum of the stem effect originated in the various experimental conditions, in-situ spectral measurements were performed using a VIS-UV compact spectrometer. It consisted in a thermoelectric cooled back-thinned CCD array (PrimeTM X, B&WTec Inc, USA) operating within a wavelength range 200–990 nm. An inline filter holder (B&W Tek Inc., DE, USA) was used to place the filter F2.

Figure 2. Exradin W1 calibration plate with the optical fiber dosimeter in the short fiber configuration (left) and long fiber configuration (right).

2.4. Dose response and dose rate dependence

The dose response of the RL fibers was investigated in the range between 1 cGy and 7 Gy at 350 MU/min, by irradiating the fibers in a PMMA slab phantom at a 10 cm depth.
Dose rate dependence was tested with two procedures. First, we checked the Al_2O_3:C RL response on the ten dose rates given by the LINAC, ranging from 140 to 1400 MU/min (100 MU). It was performed in reference conditions with the Varian Trilogy accelerator in FFF mode. Once Varian accelerators do not change the dose per pulse but the number of pulses per unit time, this test did not truly check the dose-rate dependence. Because of that, we also performed measurements changing the source-detector distance (SDD). We performed measurements at twelve SDDs, corresponding to a range in dose rate from 17 to 200 cGy/min (FF mode). By comparing the deviation

between the RL signal in respect to the Inverse Square Law (ISL) one can analyze changes attributed to dose-rate dependence.

2.5. Output factors

Output factors of different fields generated by both the accelerators were measured. In detail, the fibers were irradiated to 100 MU using a 6 MV photon beam (Elekta) at a 10 cm depth in PMMA (90 cm SSD) with field sizes ranging from 3 x 3 cm^2 to 30 x 30 cm^2. Similar tests were performed in FFF mode, 100 MU, 6 MV photon beam (Varian) using field sizes from 1 x 1 cm^2 to 10 x 10 cm^2 with the fibers placed in the water phantom.

2.6. Transversal beam profile

The transverse beam profile of a 6 MV photon beam of size 10x 10 cm^2 was measured by placing the dosimeter in the PMMA slab phantom at the depth of 10 cm and by changing its transverse distance from the center of the radiation field, as shown in Figure 3. Due to the asymmetric configuration used, the dosimeter was moved by keeping the fiber axis parallel to the profile axis. Therefore, the portion of fiber in the beam changed while measuring the profile. In this set-up, the contribution of stem effect was expected to be maximized at one side of the outer region of the profile and minimized at the opposite direction. For each position, 100 MU were delivered at 350 MU/min in FF mode.

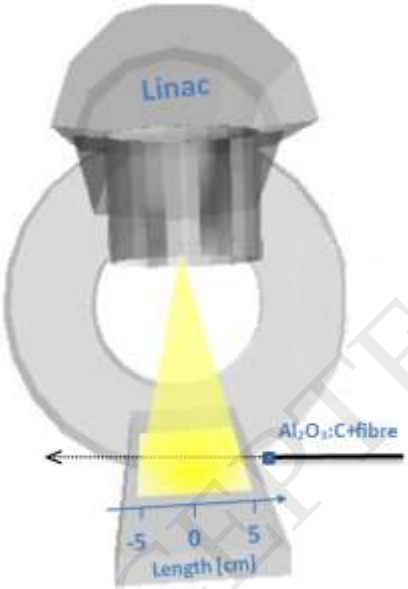

Figure 3. Sketch of the beam profile irradiations, where the fibers were irradiated at different points relative to the beam axis. Measurements were made out-of-field and in-field, along an axis parallel to the patient table. The sketch does not show the slab phantom for sake of figure simplicity.

2.7. Percentage depth-dose profile

To obtain the percentage depth–dose (PDD) curves we placed the dosimeter+fibers at different depths in the water phantom. The system was calibrated at 10 cm, so any depth-dependent features would be relative to that depth. For each depth position, the fibers were irradiated to 100 MU at 350 MU/min in FF mode, using a field of size 10x10 cm^2 generated by the Elekta accelerator.

3. Results and discussion

3.1. RL signal and stem effect

Figure 4 shows an example of RL signal versus time, measured with the Al_2O_3:C '38μm' dosimeter irradiated to 6 MV (1400 MU/min). The rise and fall of the signal occur at the radiation beam switching on and off, respectively. The amplitude of RL curve and its integral (i.e. total counts recorded during the irradiation time, after the subtraction of the instrumental background) are directly related to the dose rate and to the dose, respectively. It is worth noting that dosimeter maintains a constant RL intensity level over the entire irradiation period. This evidence validates the procedure of pre-saturation of the dosimeters for removing possible memory effects.
At the end of the irradiation, a slight after-glow is visible in the RL vs. time curve, but the signal returns to the background level within approximately 1.5 seconds. Therefore, the consequence of this phenomenon on the practical use of the dosimeter can be considered of slight importance, since it implies an increase in the background contribution that must be subtracted from the total counts, only when repeated measurements are performed in a very short time.

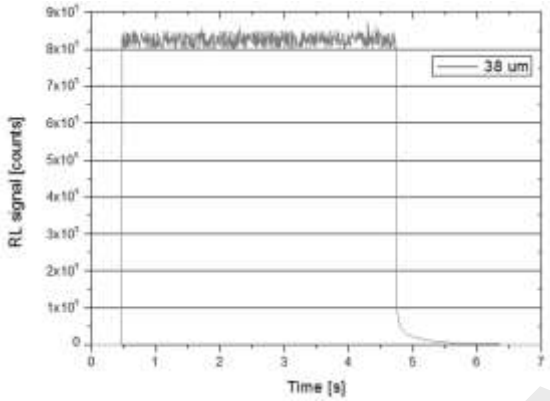

Figure 4. RL signal versus time, measured with the Al_2O_3:C '38μm' dosimeter irradiated to 6 MV (1400 MU/min).

Figure 5 shows the RL spectra of the Al_2O_3:C single crystal dosimeter measured in the short and long fiber configuration (Figure 2) using the spectrometer mounting the filter F2. In spite of the high scintillation efficiency of the dosimeter, the RL signal in the long configuration was almost double compared with the short one, because of the contribution of the stem effect. This finding confirmed the need to use a temporal discrimination scheme, in addition to the filtering system, to efficiently remove the stem effect. Therefore, in order to reduce the stem effect we used together the F2 set of filters and a sampling rate of 200 Hz.

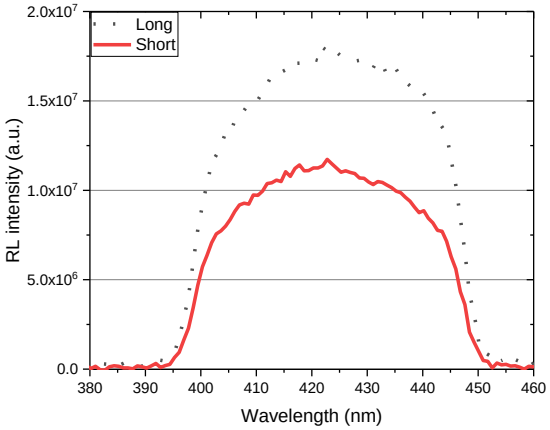

Figure 5. RL emission of the 'CG fiber' irradiated to 1400 MU/min in the long and short fiber configuration (see figure 2). The filter (F2) was mounted in front of the spectrometer.

The differences in the RL intensities measured in the long and short configurations (see figure 2) using different dose rates are shown in Figure 6.

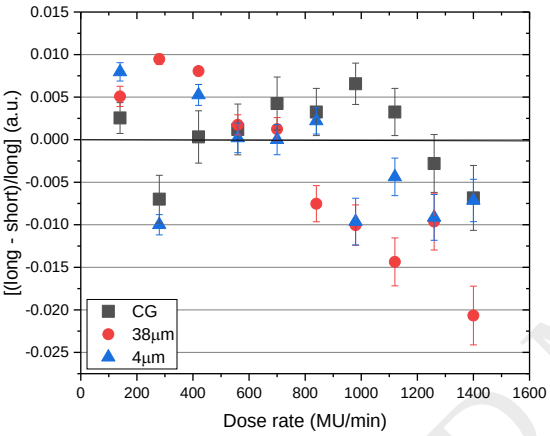

Figure 6. Differences in the RL signal acquired for fiber 'CG', '38um' and 4'um' at two different fiber configurations: short and long.

The results show that, comparing the long and short configuration, the stem effect does not have a strong contribution, with the largest deviation around 2% in case of '38um' at 1400 MU/min. In average, the deviations are below ±1%, with no specific trend for highest RL signal under long fiber configuration, compared to short.

The influence of the stem effect, on the RL signal in Al_2O_3:C fiber dosimeters, has been investigated by several authors [46-48]. As a consensus, a complete spectral separation of the two signals is complicated, but a significant reduction of the stem effect can be obtained by proper selection of filters and by gated dosimetric measurements (in a pulsed mode).

3.2. Dose response and dose rate dependence

Figure 7 shows the relationship between measured dose vs. given dose for 'CG', '38μm', and '4μm' dosimeters. In all the cases, the curve is linear up to 5 Gy, and above that, the three fibers present a supralinear behavior, which is more visible for 'CG' and slightly visible for '4μm'.

Al_2O_3:C RL dose deviations from linearity are generally explained in terms of filling of deep electron and hole traps that compete for the capture of free charges during either irradiation or readout stage [49].

Both Jursinic [50] and Andersen [28] reported a small supralinearity for irradiations with a 6 MV photon beam for doses around 2 Gy. Yukihara et al [51] also noticed a small supralinearity in OSL

Luxel™ dosimeters for doses above ~5 Gy using as readout system a Risø TL/OSL reader [52]. These observations are consistent with the dose response presented in Figure 7 and suggest that supralinearity is intrinsic of the Al_2O_3:C material for RL and OSL signals.

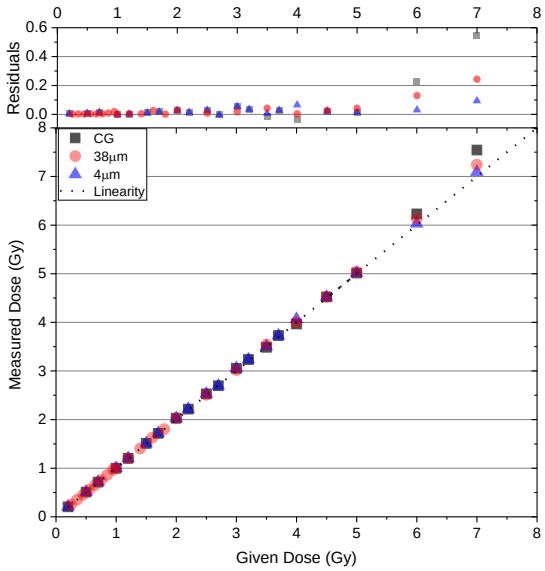

Figure 7. Measured dose with the 'CG' (squares), '38um' (dots) and '4um' (triangles) dosimeters irradiated with doses from 0.1 to 7 Gy and compared to reference values (dashed lines). Upper graph presents the deviations with respect to the expected linear dose response. Error bars are smaller than the size of the symbols.

For each fiber type, the dependence of the RL intensities on the dose rates available in the FFF modality is shown in Figure 8. In Figure 9 the normalized integrated RL signals for each irradiation with 100 MU (i.e. dose) are plotted versus the dose rate. Dose rate dependency is observed for the 'CG' fibre, for dose rates smaller than 900 MU/min. '38um' fibre also presents dose rate dependence for doses rates smaller than 900MU/min, but with nearly half contribution when compared with 'CG'. The '38um' fibre presents a consistent dose vs dose rate line with no apparent over or underresponse compared to the lowest dose rate (140 MU/min).

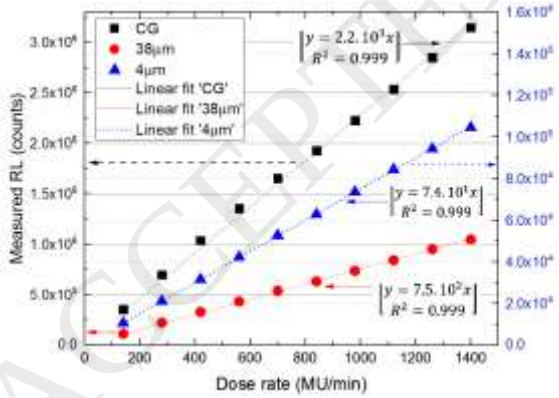

Figure 8. Dose rate dependence for '38µm', '4µm' and 'CG' fibers irradiated with 100 MU (10 cm x10 cm, SSD 90 cm, 10 cm depth) in a range of dose rates from 140 to 1400MU/min (FFF mode). Measured RL from '4um' is represented in the "Y" axis from the right side for better visualization.

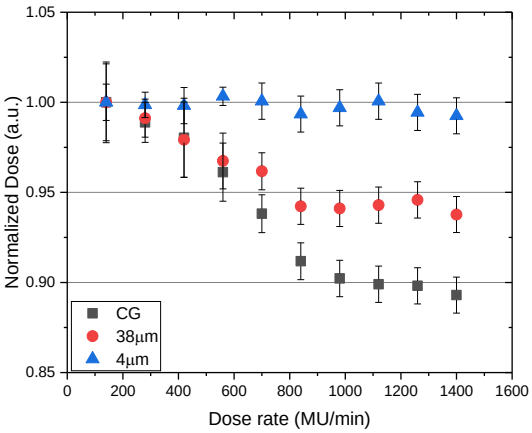

Figure 9. Normalized total integrated RL counts (i.e. dose) vs dose rate (MU/min) for fibers 'CG', '38um' and '4um'.

The results of the RL measurements carried out by changing the SSD are shown in Figure 10 for 'CG' and '38um' in FF mode (from 170 to 2000 cGy/min). In both 'CG' and '38um' a similar trend is observed, with the fiting close the expected x^{-2} shape ($x^{-1.94}$ for both fibers). The lowest dose rate, 17 cGy/min (239 cm), was acquired with the fibre at the floor of the treatment room. At this condition one expect that the scattering radiation coming from the floor has some significant contribution. Al_2O_3:C has overresponse for low energies, due to its high Z_{eff}. This overresponse is probably the reason why the fiting deviates a little bit from the expected value.

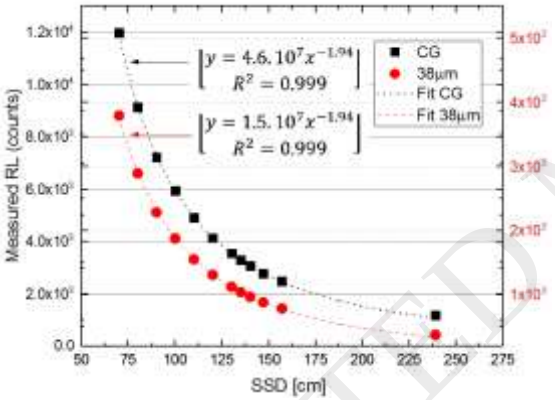

Figure 10. Dose rate dependence for '38um' and CG fiber irradiated with 100 MU by changing the source-detector distance (SDD). Error bars are smaller than the size of the symbols. "Y"-axis for '38um' is presented in the right side of the figure.

3.3. Output factors

The output factors (OF) of 6 MV photon fields with size from 3x3 cm^2 up to 30x30 cm^2 generated by the Elekta accelerator and measured with the '38μm' and 'CG' dosimeters are shown in Figure 11. The data obtained with the optical fiber dosimeters are compared with the reference values provided by the ionization chambers. The highest deviation of approximately 1.5 % was found at 3x3 cm^2 for 'CG'.

The results of output factors measurements of the photon fields produced by the Varian accelerator with respect to field size are presented in Figure 12. In such case, the plastic scintillator Exradin W1 was assumed as the reference dosimeter. The residuals of the OFs obtained using the '38μm' and 'CG' detectors with respect to the W1 scintillator were calculated and shown in the upper part of Figure 12.

Respect to the reference, the OFs obtained with the 'CG' dosimeter showed a systematic over-response from 2% up to nearly 6% for the smallest field size in the range from 30 to 10 mm.

On the other hand, the OF values measured with the '38μm' dosimeter agree with the reference ones within 1% for all the investigated field sizes. It suggests that, in the performed measurements, the reduced dimensions of the dosimeter that can be considered point-like can partially compensate the over-response due to the non-water equivalence of Al_2O_3:C.

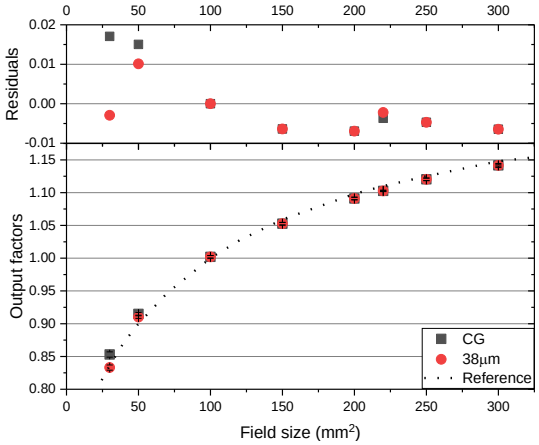

Figure 11. Output factors from '38μm' and 'CG' fiber radioluminescence signals (RL) for different field sizes compared to reference data obtained with ionization chambers (dashed line). Irradiations were carried out with 6 MV photon beam, FF, at 10 cm depth in water, from 30 x 30 to 300 x 300 mm² (Elekta Compact).

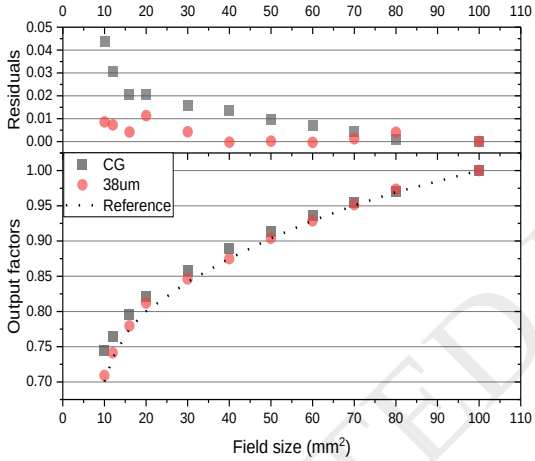

Figure 12. Output factors calculated from 'CG' and '38μm' radioluminescence signals (RL) for different field sizes compared to reference data obtained with scintillator fiber (dashed lines). Irradiations were carried out with 6 MV photon beam, FFF, at 10 cm depth in water, 10 x 10 to 100 x 100 mm² (Varian Trilogy).

3.4. Dose profile

Figure 13 presents the beam profile for 'CG' and '38μm' fibers, in a 10 x 10 cm² irradiation field. The relative RL measurements are compared with the RL emission measured at the center of the main beam, as one can see in Figure 3. That means that at position +5 cm the tip of the optical fiber is in the penumbra region, with almost no optical fiber been irradiated by the direct beam, while, at -5 cm the tip of the fiber (where the crystal of droplet is glued) is again in the penumbra region and 10 cm of fiber is been irradiated by the main beam (+5cm, -5cm).
The stem effect increases with respect to the portion of fiber been irradiated. As comparison, a bare fiber was irradiated in the same conditions and a clear difference can be seen in Figure 14, where the signal at -5 cm is >4 times higher than at +5cm. We don't find such difference in Figure 13, although is clear that, for the single crystal probe ('CG') the size of the detectors plays an important role on the spatial resolution, giving the higher residuals at the penumbra and out of field regions, when compared with '38μm'.

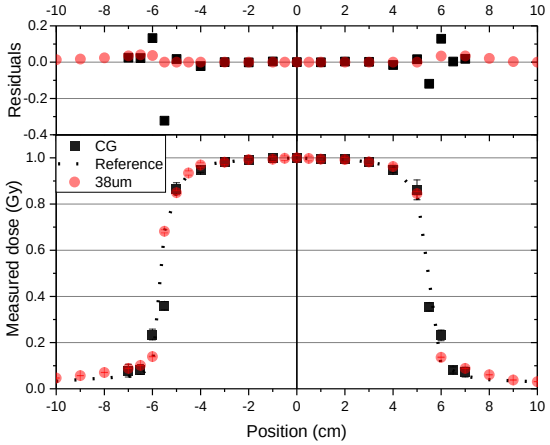

Figure 13. Profile for 'CG' and '38um' fibers according to the sketch of Figure 3. Fibers are irradiated with 10x10 cm^2 6 MV photons (1 Gy) along the profile and the results are compared to reference data (dashed line). The upper graph shows the residuals.

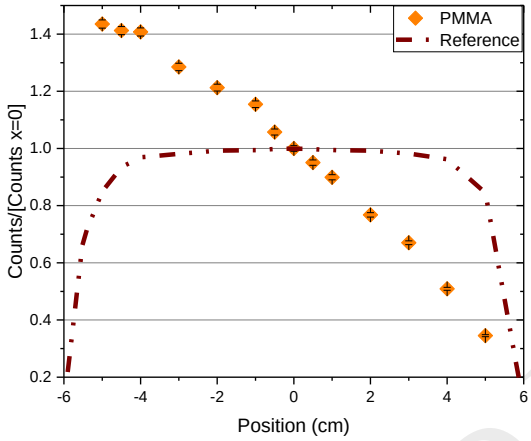

Figure 14. Profile for bare fiber according to the sketch of Figure 3. PMMA fiber is irradiated with 10x10 cm^2 6 MV photons (1 Gy) along the profile.

3.5. Percentage depth-dose profile

Figure 15 shows the results of the PDD curves for '38µm' and 'CG'. For '38µm', the standard deviations between the measurements and the hospital reference data have a highest value lower than 1% and average of 0.5%. The PDD curves did not indicate any systematic change in the RL-response with depth and the data points reproduce the reference curve within the dosimeter uncertainty.

'CG' have similar results. In this case, the deviations between 'CG' and the reference data are higher compared to '38µm (i.e. maximum deviation of 2.3% and average of 1 %).

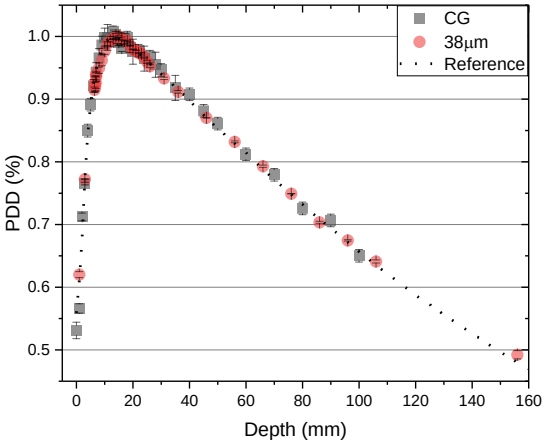

Figure 15. 6 MV percentage depth–dose curve measured in water phantom with the 'CG' and '38μm' fiber. Each of the 37 irradiations corresponded to 100 MU, 350 MU/min, FF, 10 cm x 10 cm (1 Gy).

3.6. Comparison between single crystal and droplet fibers

Using droplet or single crystal coupled to an optical fiber presented good results in the tests concerning its clinical use as a real time dosimeter system. However, the droplet has better results and gives the advantage of a 200 μm detector, i.e., with a high spatial resolution. The droplet size can be further diminished, and such size would be difficult to obtain using a single crystal.

For dosimetry in narrow photons beams, air filled ionization chambers generally have such sizes that the volume averaging effect is not negligible when the field size approach the lateral charged particle equilibrium distance. Al_2O_3:C radioluminescence detectors coupled to optical fibers can represent an advantageous solution thanks to the higher spatial resolution; nevertheless they are not water equivalent and their higher photoelectric effect cross section make their response dependent on the spectral composition of the radiation beam. As a consequence the over-response from low energy photons (< 100 keV) might be overestimated by RL detectors based on Al_2O_3:C affecting significantly the dose estimation. This effect was noted in this study for the larger CG detector when approaching the not charged particle equilibrium field sizes, but its magnitude became negligible using the point-like 38μm detector .

Regarding the evidence difference for difference grain sizes, for instance for dose rate dependency (Figure 9), our supposition is that this effect comes from the competition between immediate recombination of charge carriers and trapping of charge. Al_2O_3:C was not initially designed for RL or scintillating applications, but for trapping and storage, having a lot of trapping centers.

In the single crystal ('CG') and large powder grains (such as '38um'), charge can drift further away and be trapped reducing the probability of immediate recombination at high dose rates, when the traps are saturated very quickly. Small grains ('4um'), in turn, will prevent charges from drifting away and will result faster saturation of traps and constant RL as a function of dose rate. Although our fibers were pre-irradiated with a high dose to account for trap competition, this was not enough for larger grain sizes. We expect that, for bleached detectors the effect is even larger. Next step of our work will focus on the simulation of this effect, to compare with our measurements.

3.7. Conclusions

The measurements reported in this work confirm the suitability of Al_2O_3:C radioluminescence detectors coupled to optical fibers for clinical dosimetry in a wide range of settings including small field sizes. Its features compare favorably with those of ion chamber systems. In fact, the high sensitivity of Al_2O_3:C permits to prepare small size droplets based on Al_2O_3:C thin powder mixed with a photocurable polymer. These droplets are suitable for accurate determination of doses, in real

time, from 0.1 to 5 Gy, percentage depth dose and transverse profiles. When output factors of different field sizes are compared, '38μm' fiber presents a good agreement with the reference data obtained with two difference ionization chambers and a fiber scintillator. Its tissue non-equivalence can be compensate minimizing the detector size.
Nevertheless, there are some drawbacks to be considered in the use of such prototype, 1) each detector-fiber has a different sensitivity (due to amount of material and distribution of F-centers in the crystal), so each fiber needs an individual calibration, while once calibrated the detector+fiber can be used several times before re-calibration is needed, and 2) preference should be given to small grain sizes, where better results were observed.

4. Acknowledgements

The authors would like to thank Dr. Mark Akselrod (Landauer Inc.) for the valuable discussion about the Al_2O_3:C properties.

5. References

[1] G. Budgell, K. Brown, J. Cashmore, S. Duane, J. Frame, M. Hardy, et al., IPEM topical report 1: guidance on implementing flattening filter free (FFF) radiotherapy, Physics in Medicine and Biology, 61(2016) 8360.
[2] R. Alfonso, P. Andreo, R. Capote, M.S. Huq, W. Kilby, P. Kjäll, et al., A new formalism for reference dosimetry of small and nonstandard fields, Medical physics, 35(2008) 5179-86.
[3] P. Charles, G. Cranmer-Sargison, D.I. Thwaites, S. Crowe, T. Kairn, R. Knight, et al., A practical and theoretical definition of very small field size for radiotherapy output factor measurements, Medical physics, 41(2014).
[4] I.J. Das, G.X. Ding, A. Ahnesjö, Small fields: nonequilibrium radiation dosimetry, Medical physics, 35(2008) 206-15.
[5] H. Bouchard, J. Seuntjens, Ionization chamber-based reference dosimetry of intensity modulated radiation beams, Medical physics, 31(2004) 2454-65.
[6] F. Moretti, G. Patton, A. Belsky, M. Fasoli, A. Vedda, M. Trevisani, et al., Radioluminescence Sensitization in Scintillators and Phosphors: Trap Engineering and Modeling, The Journal of Physical Chemistry C, 118(2014) 9670-6.
[7] A.S. Saini, T.C. Zhu, Dose rate and SDD dependence of commercially available diode detectors, Medical physics, 31(2004) 914-24.
[8] N. Knutson, H. Li, V. Rodriguez, Y. Hu, R. Kashani, H. Wooten, et al., SU-ET-494: A MOSFET-Based In-Vivo Dosimetry System for MR Image-Guided Radiation Therapy (MR-IGRT), Medical Physics, 41(2014) 340-.
[9] J. Boivin, S. Beddar, M. Guillemette, L. Beaulieu, A novel tool for in vivo dosimetry in diagnostic and interventional radiology using plastic scintillation detectors, World Congress on Medical Physics and Biomedical Engineering, June 7-12, 2015, Toronto, Canada, Springer2015, pp. 680-4.
[10] N. Chiodini, A. Vedda, M. Fasoli, F. Moretti, A. Lauria, M.C. Cantone, et al., Ce-doped SiO2 optical fibers for remote radiation sensing and measurement, SPIE Defense, Security, and Sensing, International Society for Optics and Photonics2009, pp. 731616--8.
[11] B. Mijnheer, I. Olaciregui-Ruiz, R. Rozendaal, H. Spreeuw, M. van Herk, A. Mans, Current status of 3D EPID-based in vivo dosimetry in The Netherlands Cancer Institute, Journal of Physics: Conference Series, IOP Publishing2015, p. 012014.
[12] B. Mijnheer, S. Beddar, J. Izewska, C. Reft, In vivo dosimetry in external beam radiotherapy, Medical physics, 40(2013) 070903.
[13] R.P. Patel, A.J. Warry, D.J. Eaton, C.H. Collis, I. Rosenberg, In vivo dosimetry for total body irradiation: five-year results and technique comparison, Journal of Applied Clinical Medical Physics, 15(2014) 4939.

[14] A.S. Beddar, S. Law, N. Suchowerska, T.R. Mackie, Plastic scintillation dosimetry: optimization of light collection efficiency, Physics in medicine and biology, 48(2003) 1141.
[15] Y. Hu, Z. Qin, Y. Ma, W. Zhao, W. Sun, D. Zhang, et al., Characterization of fiber radiation dosimeters with different embedded scintillator materials for radiotherapy applications, Sensors and Actuators A: Physical, (2017) 7.
[16] G.A. Mahdiraji, M. Ghomeishi, E. Dermosesian, S. Hashim, N. Ung, F.M. Adikan, et al., Optical fiber based dosimeter sensor: beyond TLD-100 limits, Sensors and Actuators A: Physical, 222(2015) 48-57.
[17] A. Beddar, T. Mackie, F. Attix, Water-equivalent plastic scintillation detectors for high-energy beam dosimetry: I. Physical characteristics and theoretical considerations, Physics in Medicine & Biology, 37(1992) 1883.
[18] L.A. Benevides, A.L. Huston, B.L. Justus, P. Falkenstein, L.F. Brateman, D.E. Hintenlang, Characterization of a fiber-optic-coupled radioluminescent detector for application in the mammography energy range, Medical physics, 34(2007) 2220-7.
[19] R. Nowotny, Radioluminescence of some optical fibres, Physics in Medicine & Biology, 52(2007) N67.
[20] I. Veronese, N. Chiodini, S. Cialdi, E. D'Ippolito, M. Fasoli, S. Gallo, et al., Real-time dosimetry with Yb-doped silica optical fibres, Physics in medicine and biology, 10(2017) 4218-36.
[21] I. Veronese, M. Cantone, N. Chiodini, M. Fasoli, E. Mones, F. Moretti, et al., The influence of the stem effect in Eu-doped silica optical fibres, Radiation Measurements, 56(2013) 316-9.
[22] E. Cruz-Zaragoza, C. Furetta, J. Marcazzó, M. Santiago, C. Guarneros, M. Pacio, et al., Thermoluminescence and radioluminescence properties of tissue equivalent Cu-doped Li2B4O7 for radiation dosimetry, (2015).
[23] A.K.M. Mizanur Rahman, M. Begum, H. Zubair, H. Abdul-Rashid, Z. Yusoff, N. Ung, et al., Ge-doped silica optical fibres as RL/OSL dosimeters for radiotherapy dosimetry, Sensors and Actuators A: Physical, 264(2017) 30-9.
[24] C. Jiang, P. Deng, J. Zhang, F. Gan, Radioluminescence of Ce3+-doped B2O3–SiO2–Gd2O3–BaO glass, Physics Letters A, 323(2004) 323-8.
[25] A.R. Beierholm, C.E. Andersen, L.R. Lindvold, F. Kjær-Kristoffersen, J. Medin, A comparison of BCF-12 organic scintillators and Al2O3:C crystals for real-time medical dosimetry, Radiation Measurements, 43(2008) 898-903.
[26] S. Beddar, L. Beaulieu, Scintillation dosimetry: CRC Press; 2016.
[27] A.M.C. Santos, M. Mohammadi, S. Afshar, Investigation of a fibre-coupled beryllium oxide (BeO) ceramic luminescence dosimetry system, Radiation Measurements, 70(2014) 52-8.
[28] C. Andersen, M. Aznar, L. Bøtter-Jensen, S. Bäck, S. Mattsson, J. Medin, Development of optical fibre luminescence techniques for real time in vivo dosimetry in radiotherapy, IAEA, Vienna, 2(2003) 353-60.
[29] L. Nascimento, F. Vanhavere, E. Boogers, J. Vandecasteele, Y. De Deene, Medical Dosimetry Using a RL/OSL Prototype, Radiation Measurements, (2014).
[30] A. Viamonte, L. Da Rosa, L. Buckley, A. Cherpak, J. Cygler, Radiotherapy dosimetry using a commercial OSL system, Medical physics, 35(2008) 1261-6.
[31] M. Akselrod, A. Lucas, J. Polf, S. McKeever, Optically stimulated luminescence of Al2O3, Radiation measurements, 29(1998) 391-9.
[32] A. Peto, A. Kelemen, Radioluminescence properties of alpha-Al2O3 TL dosemeters, Radiation protection dosimetry, 65(1996) 139-42.
[33] G. Erfurt, M. Krbetschek, T. Trautmann, W. Stolz, Radioluminescence (RL) behaviour of Al2O3:C-potential for dosimetric applications, Radiation measurements, 32(2000) 735-9.
[34] C. Andersen, C. Marckmann, M. Aznar, L. Bøtter-Jensen, F. Kjær-Kristoffersen, J. Medin, An algorithm for real-time dosimetry in intensity-modulated radiation therapy using the radioluminescence signal from Al2O3: C, Radiation protection dosimetry, 120(2006) 7-13.

[35] C.E. Andersen, S.M.S. Damkjær, G. Kertzscher, S. Greilich, M. Aznar, Fiber-coupled radioluminescence dosimetry with saturated Al2O3:C crystals: Characterization in 6 and 18 MV photon beams, Radiation Measurements, 46(2011) 1090-8.
[36] F. Klein, S. Greilich, C.E. Andersen, L.R. Lindvold, O. Jäkel, A thin layer fiber-coupled luminescence dosimeter based on Al 2 O 3: C, Radiation Measurements, 46(2011) 1607-9.
[37] L. Nascimento, F. Vanhavere, E. Boogers, J. Vandecasteele, Y. De Deene, Medical dosimetry using a RL/OSL prototype, Radiation Measurements, 71(2014) 359-63.
[38] L. Nascimento, F. Vanhavere, S. Kodaira, H. Kitamura, D. Verellen, Y. De Deene, Application of Al 2 O 3: C+ fibre dosimeters for 290MeV/n carbon therapeutic beam dosimetry, Radiation Physics and Chemistry, 115(2015) 75-80.
[39] G. Ranchoux, S. Magne, J. Bouvet, P. Ferdinand, Fibre remote optoelectronic gamma dosimetry based on optically stimulated luminescence of Al2O3: C, Radiation protection dosimetry, 100(2002) 255-60.
[40] L. Nascimento, C. Saldarriaga, F. Vanhavere, E. D'Agostino, G. Defraene, Y. De Deene, Characterization of OSL Al 2 O 3: C droplets for medical dosimetry, Radiation Measurements, 56(2013) 200-4.
[41] L. Nascimento, C. Saldarriaga, F. Vanhavere, E. D'Agostino, G. Defraene, Y. De Deene, Characterization of OSL Al2O3:C droplets for medical dosimetry, Radiation Measurements, 56(2013) 200-4.
[42] A.K.M. Mizanur Rahman, M. Begum, M. Begum, H. Zubair, H. Abdul-Rashid, Z. Yusoff, et al., Radioluminescence of Ge-doped silica optical fibre and Al2O3: C dosimeters, Sensors and Actuators A: Physical, 270(2018) 72-8.
[43] S. Damkjær, C.E. Andersen, Memory effects and systematic errors in the RL signal from fiber coupled Al2O3: C for medical dosimetry, Radiation Measurements, 45(2010) 671-3.
[44] S. Agostinelli, S. Garelli, M. Piergentili, F. Foppiano, Response to high-energy photons of PTW31014 PinPoint ion chamber with a central aluminum electrode, Medical physics, 35(2008) 3293-301.
[45] J. Pena, F. Sánchez-Doblado, R. Capote, J. Terrón, F. Gómez, Monte Carlo correction factors for a Farmer 0.6 cm3 ion chamber dose measurement in the build-up region of the 6 MV clinical beam, Physics in medicine and biology, 51(2006) 1523.
[46] C.J. Marckmann, M.C. Aznar, C.E. Andersen, L. Bøtter-Jensen, Influence of the stem effect on radioluminescence signals from optical fibre Al2O3: C dosemeters, Radiation protection dosimetry, 119(2006) 363-7.
[47] K.J. Jordan, Evaluation of ruby as a fluorescent sensor for optical fiber-based radiation dosimetry, Photonics West'96, International Society for Optics and Photonics1996, pp. 170-8.
[48] B.L. Justus, P. Falkenstein, A.L. Huston, M.C. Plazas, H. Ning, R.W. Miller, Gated Fiber-Optic-Coupled Detector for In Vivo Real-Time Radiation Dosimetry, Applied optics, 43(2004) 1663-8.
[49] E. Yukihara, V. Whitley, S. McKeever, A. Akselrod, M. Akselrod, Effect of high-dose irradiation on the optically stimulated luminescence of Al2O3:C, Radiation measurements, 38(2004) 317-30.
[50] P.A. Jursinic, Characterization of optically stimulated luminescent dosimeters, OSLDs, for clinical dosimetric measurements, Medical physics, 34(2007) 4594-604.
[51] E. Yukihara, G. Mardirossian, M. Mirzasadeghi, S. Guduru, S. Ahmad, SU-FF-T-248: Improved Accuracy in Radiotherapy Dosimetry of High-Energy Photon and Electron Beam Using Optically Stimulated Luminescence, Medical Physics, 34(2007) 2458-.
[52] L. Bøtter-Jensen, E. Bulur, G.A.T. Duller, A.S. Murray, Advances in luminescence instrument systems, Radiation Measurements, 32(2000) 523-8.

Author biography

Luana de Freitas Nascimento – has a bachelor and M.Sc. in Physics from the University of Sao Paulo, Brazil, and also has received a double Ph.D. degree from Ghent University and Vrije Universiteit Brussel (VUB) in 2015. Currently, she is a Research Fellow at the Radiation Protection Dosimetry and Calibration group from the Belgian Nuclear Research Centre, Belgium. Her research interests are focused on the medical dosimetry especially on luminescence dosimetry techniques.

Ivan Veronese - is Assistant Professor at the Department of Physics of the University of Milan. He achieved his Master of Science in Physics and Ph.D. in Physics, Astrophysics and Applied Physics. His research is conducted in the field of applied physics of ionizing radiation with particular focus on dosimetry and radiation protection. He is full member of the Working Group on Retrospective Dosimetry of the European Radiation Dosimetry Group (EURADOS); of the Italian Association of Medical Physics (AIFM); and of the National Institute of Nuclear Physics (INFN). He is in the editorial board of *Physica Medica:* European Journal of Medical Physics, reviewer for several international journals and author of more than 60 publications in peer reviewed international journals and more than 100 contributions to conferences.

Gianfranco Loi - is a senior medical physicist at Medical Physics Department of the University Hospital of Novara. He achieved his Master of Science in Physics and the post-graduation Master in Medical Physics from the University of Milan. Now he leads the medical physics team supporting the local University Radiation Oncology Department and a network of three other regional radiotherapy services. His main activities and research areas are: small field dosimetry, stereotactic ablative radiotherapy, image guided adaptive radiotherapy, deformable image registration and quantitative imaging for treatment planning optimization.

Eleonora Mones - is a medical physicist at Medical Physics Department of the University Hospital of Novara. He achieved his Master of Science in Physics from the University of Milan and the post-graduation Master in Medical Physics from the University of Turin. Her main activities and research area are related both to brachytherapy and external radiotherapy, with particular emphasis to the dosimetric issues. She is lecturer of courses of quality assurance in radiotherapy at the Faculty of Medicine of the University of Eastern Piedmont Amedeo Avogadro and member of the Italian Association of Medical Physics (AIFM).

Filip Vanhavere – has degree of civil engineering and nuclear engineering from Ghent University, and received my PhD in applied physics also at Ghent University in 1999. Head of Expert Group Radiation Protection Dosimetry and Calibration at the Belgian Nuclear Research Centre SCK•CEN, and Vice-director of the Institute Environment, Health and Safety from SCK•CEN. Vice chair of EURADOS, Secretary of MELODI.

Dirk Verellen – is department head of Medical Physics Radiotherapy in the Iridium Kankernetwerk Antwerpen and is Professor of Biomedical Physics within the Faculty of Medicine and Pharmacy of the Vrije Universiteit Brussel (VUB). He has a PhD in Medical Sciences from the Vrije Universiteit Brussel (VUB). His main field of interest is in the practical issues concerning implementation of high precision conformal radiotherapy and image-guidance in a clinical environment, also, establishing a safety culture in radiation oncology.